View metadata, citation and similar papers at core.ac.uk
brought to you by CORE
provided by Repositorio da Producao Cientifica e Intelectual da Unicamp

JOURNAL OF Materials CHEMISTRY

Preparation of the conducting nanocomposites using molded inorganic matrix: fibrous cerium(IV) hydrogenphosphate as a self-supported pyrrole polymerization agent

Carla Veríssimo and Oswaldo L. Alves*

LQES–Laboratório de Química do Estado Sólido, Instituto de Química, Unicamp, CP 6154, Campinas, SP, Brazil, CEP 13083-970. E-mail: oalves@iqm.unicamp.br; http://lqes.iqm.unicamp.br

Received 25th November 2002, Accepted 26th March 2003
First published as an Advance Article on the web 11th April 2003

New supported polypyrrole nanocomposites have been prepared and studied in this work. Self-supported sheets of fibrous cerium(IV) hydrogenphosphate (CeP_f) were used as the inorganic matrix, since the fibrous morphology presented by this material makes molding possible, giving a desired shape to the final polypyrrole/CeP_f conducting nanocomposites. The influence of pyrrole concentration on the nanocomposite preparation was studied, as well as the influence of CeP_f on the polypyrrole characteristics. XRD, Raman, SEM and conductivity measurement data show the conducting polypyrrole coating CeP_f fibers, yielding self-supported sheets of organic–inorganic conducting nanocomposites.

Published on 11 April 2003. Downloaded by UNIVERSIDAD ESTADUAL DE CAMPINAS on 05/09/2014 17:47:14.

Introduction

Nanocomposite materials have been the target of growing interest owing to their unique optical, electrical, mechanical, thermal, and magnetic properties arising from the combination of the different constituents on a nanometric scale.[1–7] In recent years, several organic–inorganic nanocomposites have been prepared by combining organic polymers and inorganic materials, employing different methods. In some cases, a polymer is introduced into the free spaces of the inorganic compound, such as the channels in zeolites, the pores in glass matrices, the interlayer spaces in layered solids, *etc.*[7–10] The introduction of monomer molecules and their further polymerization in confined environments can also be performed.[2,3,10–17] Another approach involves the coating of core-like particles of inorganic oxides, glass fibers, *etc*. This can be achieved either by adsorption of polymers on the particles or by adsorption of monomers in the cores, followed by polymerization.[18–21]

Conducting polymers are interesting materials owing to their electrical properties and their potential applications in several technological fields.[4–7,15*b*,18,22–24] Belonging to this class, polypyrrole (PPy) is one of the most studied conducting polyheterocycles. It presents relatively good air-stability and has potential uses in batteries,[25] conducting composites,[4,12,18] electrodes,[26] photoelectrochemical cells,[27] electrochemical switches,[28] sensors,[29] *etc*. Polypyrrole can be obtained in the reduced, nonconducting form, with a yellow-green color and the pyrrole rings having an aromatic-like structure. In its oxidized form, the polypyrrole lattice is distorted and the aromatic-like structure is expected to relax to a quinoid-like structure, with the formation of charged defects such as polarons and/or bipolarons on the polymer chains. In this condition, polypyrrole shows conductive properties and an intense black color.[18,20,23,24,30,31]

The potential use of polypyrrole is, however, often limited by its lack of malleability, hindering its processability.[18,20] To overcome this limitation and to obtain suitable materials, several approaches have been carried out to improve the processing capabilities, such as synthesis of β-substituted derivatives,[32] preparation of sterically stabilized polypyrrole powders,[33] and generation of conducting nanocomposites.[3,4,12,18]

The preparation of organic–inorganic nanocomposites has been regarded as an important strategy to improve the mechanical, thermal, and chemical resistance of the polymers. This type of material can also present synergic behavior between the polymer and the inorganic constituent, leading to different properties from those shown by the individual components.

Because of the wide applicability of polypyrrole, it has been used in the preparation of several nanocomposite materials over the last decade. Some examples are: i) polypyrrole-coated core particles such as SiO_2, NiO, β-Fe_2O_3, CeO_2, CuO, SnO_2, glass fibers, *etc.*;[18–21] ii) intercalated polypyrrole in zeolite Y and mordenite channels;[16,17] in the pores of Vycor glass;[12*b*,*c*,14] in interlayer spaces of MoS_2,[3] and in α-tin(IV) bis(hydrogenphosphate),[12*e*] *etc*.

This work proposes a new and interesting approach to overcome the poor processing capabilities of polypyrrole, which consists of the coating of an inorganic material—which could be previously molded into any desired shape—by the polymer, giving rise to a supported polypyrrole nanocomposite.

Cerium(IV) hydrogenphosphate (CeP) belongs to the class of acid salts of tetravalent metals, whose inorganic network is constituted by the concatenation of $M^{IV}O_6$ octahedra (M = Zr, Ti, Ce, Sn, *etc*.) and XO_4 tetrahedra (X = P or As), which are arranged to form two- and three-dimensional structures.[34,35] Several CeP have been synthesized, presenting different PO_4/Ce molar ratios, crystallinity and morphology, these characteristics being strongly dependent on the preparation conditions, such as initial PO_4/Ce molar ratio, digestion time and temperature.[36]

Usually, cerium(IV) hydrogenphosphate presents a two-dimensional structure where the cerium atoms, that constitute the layers, are connected to hydrogenphosphate groups. The strong interest in these compounds is due to their ion exchange capabilities: the proton of the hydrogenphosphate group can be easily replaced by other cations.[37,38]

CeP can present different morphologies, of which the microcrystalline is commonly observed. By controlling the experimental parameters, a fibrous morphology can be synthesized, allowing the final material to be obtained as a flexible self-supported sheet, similar to cellulose paper.[35*b*,36,37]

 DOI: 10.1039/b211594h

This journal is © The Royal Society of Chemistry 2003

View Article Online

Published on 11 April 2003. Downloaded by UNIVERSIDAD ESTADUAL DE CAMPINAS on 05/09/2014 17:47:14.

The structure of fibrous cerium(IV) hydrogenphosphate (CeP_f), however, remains unknown due to the lack of crystallites with appropriate sizes for XRD analysis.[35b,39] Some interesting properties of CeP_f are good mechanical and chemical stability, besides the high ion exchange capacity and high cationic selectivity, for Pb^{2+}, Tl^{+}, K^{+}, *etc.*, which make fibrous cerium(IV) hydrogenphosphate very attractive for the preparation of ion-exchange papers for chromatographic cation separations or inorganic membranes without a binder.[35b,36,37] Moreover, the presence of Ce(IV) ions allows redox reactions necessary for oxidative polymerization to occur.[35b,37] CeP_f is, therefore, an interesting inorganic material for the building of polypyrrole nanocomposites, mainly due to its fibrous morphology, which yields flexible sheets and makes possible the molding of the inorganic material, leading to conducting nanocomposites with the desired shape.

Herein we present a study of polypyrrole/fibrous cerium(IV) hydrogenphosphate nanocomposites, prepared *via in situ* chemical oxidation of pyrrole promoted by the reduction of Ce(IV) ions present in the inorganic matrix. Aspects related to the influence of the concentration of the pyrrole solution on nanocomposite preparation were studied, as well as the influence of the matrix on the morphological and structural characteristics of the polypyrrole and its physical–chemical properties.

Experimental

Preparation of fibrous cerium(IV) hydrogenphosphate self-supported sheets

Fibrous cerium(IV) hydrogenphosphate was prepared based on the procedure reported by Alberti *et al.*[36] An aqueous solution of ammonium cerium(IV) nitrate (350 cm^3, 0.05 mol dm^{-3}) was added dropwise to an aqueous phosphoric acid solution (350 cm^3, 6 mol dm^{-3}) with stirring at 90 $\pm$ 3 °C. The gelatinous precipitate originally formed was digested for 4 hours, keeping the temperature at 90 $\pm$ 3 °C, under constant stirring. The light yellow solid obtained was isolated by centrifugation and washed with water until the complete removal of nitrate ions. The material was then suspended in water, filtered under suction on a Büchner funnel, and dried at room temperature. The CeP_f self-supported sheet could be detached from the Büchner funnel (*ca.* 0.5 mm thick).

Preparation of polypyrrole/CeP_f nanocomposites

Nanocomposites were prepared by immersion of fibrous cerium(IV) hydrogenphosphate self-supported sheets (4 cm^2) in 10 cm^{-3} of freshly distilled pyrrole, as well as in ethanolic solutions with different pyrrole concentrations (1×10^{-1}–1×10^{-4} mol dm^{-3}), during 10 minutes, at room temperature. The impregnated sheets were dried under vacuum for 6 hours.

Analysis procedures

The P/Ce ratio in fibrous cerium(IV) hydrogenphosphate was determined as follows. About 50 mg of sample were dissolved in an aqueous sulfuric acid solution (10 cm^3, 9 mol dm^{-3}). Oxalic acid was added (8 cm^3, 0.05 mol dm^{-3}) to reduce Ce(IV) to Ce(III). Then, the solution was diluted to 50 cm^3 with distilled water and phosphate was determined as described by Bernhart *et al.*[40] To determinate cerium, 25 cm^3 of the prepared solution were diluted with distilled water and Ce(III) was determined spectrophotometrically at 253.5 nm as described by Greenhaus *et al.*[41] These measurements were made by using a HITACHI U-2000 UV-Vis spectrophotometer. Carbon and nitrogen were determined by elemental microanalyses using a Perkin-Elmer Model 2400 CHN Analyzer.

Physical measurements

X-Ray diffraction (XRD) measurements were recorded on a Shimadzu XD-3A diffractometer using Cu K_α radiation (30 kV, 20 mA), with a Ni filter, and a scan rate of 2° min^{-1} in 2θ. Raman spectra were measured on a Renishaw System 3000 Raman Imaging Microscope, using the 632.8 nm line of a He–Ne laser. Scanning electron microscopy (SEM) was performed by using a JEOL JSM T-300 Microscope. Electrical conductivity results were obtained using Contact Products INC apparatus formed by ten probes with five being aligned on each side, 10 mm from each other. The probes were covered with gold to facilitate electrical contact and possessed internal micro-springs to improve contact with irregular surfaces. Electrical resistance (R) was measured using a Keithley Model 171 multimeter, at room temperature.[42]

Results and discussion

In previous works, CeO_2 core particles were coated with polypyrrole through pyrrole chemical oxidation catalyzed by the Ce(IV) ions present in cerium dioxide, resulting in a self-coated product. This polymerization should be expected because the pyrrole redox potential is 1.2 V and the reduction potential of Ce(IV) to Ce(III) is between 1.8 and 1.3 V.[43] It was necessary, however, to employ appropriate experimental conditions to promote the polymerization, such as a reaction temperature around 100 °C for at least 4 hours.[18]

On the other hand, in the present study, when fibrous cerium(IV) hydrogenphosphate self-supported sheets were immersed in freshly distilled pyrrole, which is colorless, the immediate formation of polypyrrole was observed, since the light yellow self-supported sheets became black. The polypyrrole/CeP_f nanocomposite obtained in this way was called PPY/CeP_f-p.

The influence of the pyrrole concentration on nanocomposite preparation was also studied. In Table 1, the names of the samples and the different pyrrole concentrations in ethanolic solutions used in nanocomposite preparation are listed, including a blank sample (CeP_f-blank).

The PPY/CeP_f-1 nanocomposite exhibits behavior similar to PPY/CeP_f-p, becoming a black material, whereas the PPY/CeP_f-2, PPY/CeP_f-3 and PPY/CeP_f-4 samples just presented a small color change, from light yellow to darker yellow.

It is important to note that the self-supported sheet integrity is preserved after these experiments. This result is very interesting because the shape integrity makes the building of molded conducting devices possible.

X-Ray diffractometry

The X-ray diffraction pattern of the CeP_f self-supported sheet shows well-defined peaks in the range of 5–50° (2θ) and a peak at 7.2° (2θ), d = 12.2 Å, indicating a layered structure (Fig. 1).[36,39,44] After the inorganic matrix is brought into contact with ethanol or ethanol/pyrrole solutions, one can observe the absence of well-defined peaks, which indicates structural disorder in the CeP_f lattice. The intensity decrease of

Table 1 Sample identification and pyrrole concentration in ethanolic solutions

Sample name	Pyrrole concentration in ethanolic solutions/mol dm^{-3}
PPY/CeP_f-p	pure pyrrole
PPY/CeP_f-1	1×10^{-1}
PPY/CeP_f-2	1×10^{-2}
PPY/CeP_f-3	1×10^{-3}
PPY/CeP_f-4	1×10^{-4}
CeP_f-blank	pure ethanol

View Article Online

Published on 11 April 2003. Downloaded by UNIVERSIDAD ESTADUAL DE CAMPINAS on 05/09/2014 17:47:14.

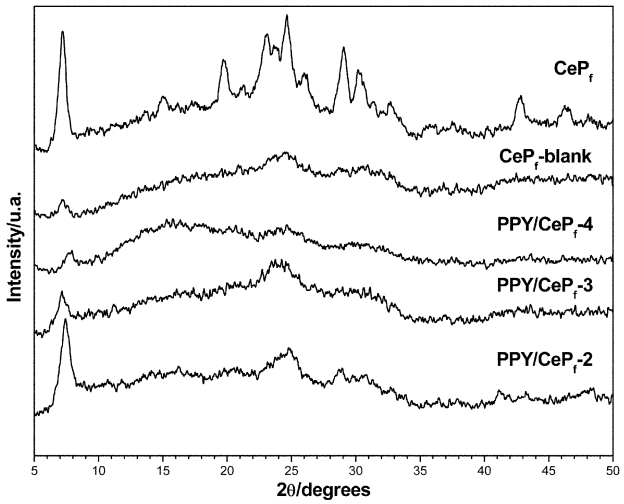

Fig. 1 X-Ray diffraction patterns of CeP$_f$, CeP$_f$-blank, PPY/CeP$_f$-4, PPY/CeP$_f$-3 and PPY/CeP$_f$-2 samples.

the peak around 7° (2θ), d = 12.6 Å, attributed to the interlayer distance, also suggests the loss of a layered stucture for the CeP$_f$-blank, PPY/CeP$_f$-3 and PPY/CeP$_f$-4 samples. On the other hand, the XRD pattern of the PPY/CeP$_f$-2 sample shows the maintenance of the peak intensity at 7.4° (2θ), d = 11.9 Å, suggesting that an increase in the pyrrole concentration enhances the stability of the CeP$_f$ layered structure. In Fig. 1 one can also observe the lack of significant changes of the interlayer distance values for the PPY/CeP$_f$-2, PPY/CeP$_f$-3 and PPY/CeP$_f$-4 nanocomposites, indicating the absence of polypyrrole or oligomer formation intercalated into the layers.

In the X-ray diffraction pattern of PPY/CeP$_f$-p and PPY/CeP$_f$-1 nanocomposites, one can observe the absence of reflection peaks associated with CeP$_f$ and the presence of several new reflection peaks, which suggest the formation of a new structural phase after CeP$_f$ has been immersed in pyrrole (Fig. 2). Changes in the XRD patterns can not be explained by polypyrrole reflections, since it possesses a low crystallinity and presents just a broad peak around 22° (2θ), d = 4.0 Å.[18a] The reduction of Ce(IV) to Ce(III) involved in the polymerization process, however, may lead to formation of cerium(III) orthophosphate. Comparing d-spacings from XRD patterns, as well as relative intensities, of PPY/CeP$_f$-p and PPY/CeP$_f$-1 nanocomposites with the literature values for cerium(III) orthophosphate (CePO$_4$) one can observe good agreement (Table 2). Therefore, when polymerization takes place, fibrous cerium(IV) hydrogenphosphate is converted to cerium(III) orthophosphate.

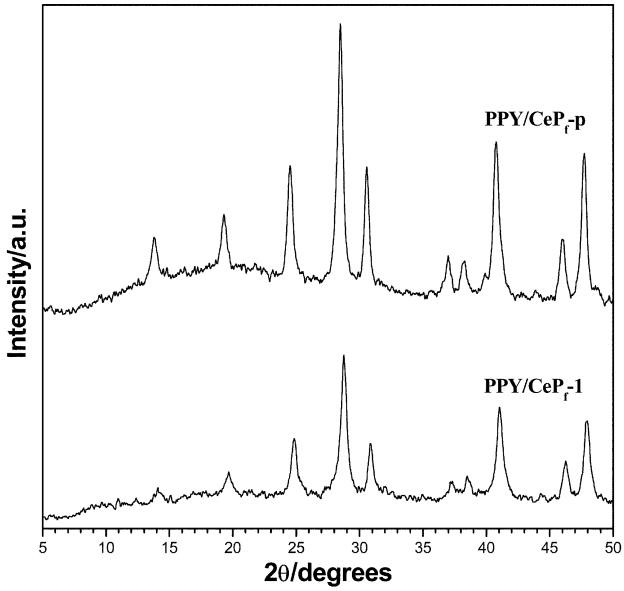

Fig. 2 X-Ray diffraction patterns of PPY/CeP$_f$-p and PPY/CeP$_f$-1 nanocomposites.

Raman spectroscopy

Since the molecular vibrations are sensitive to structural differences, Raman spectroscopy was used to confirm the presence of the oxidized polypyrrole form, owing to its different resonance structures: an aromatic structure in the reduced form and a quinoid structure in the oxidized form.

Moreover, this technique has also been employed to study the presence of polarons and/or bipolarons on polymeric chains. The first is a cation radical formed by removal of one electron from the polypyrrole chain followed by lattice relaxation, whereas the latter is a dication associated with strong local lattice distortion, whose formation is expected at high levels of doping.[30,31] These entities act as charge carriers, responsible for the conductivity of the polypyrrole, and may be considered localized structural defects on the polymeric chain.[46]

Raman spectra of PPY/CeP$_f$-p and PPY/CeP$_f$-1 nanocomposites show the absence of bands associated with CeP$_f$ vibrational modes and present bands related to the oxidized polypyrrole form, with polarons and bipolarons on the polymeric chains (Fig. 3). One can observe bands centered at 1367, 1246, 1087, and 935 cm^{-1} assigned to bipolarons, whereas the bands centered at 1059 and 970 cm^{-1} are assigned to polarons. In its reduced form, polypyrrole presents just one

Table 2 d-Spacings and relative intensities from XRD patterns of PPY/CeP$_f$-p and PPY/CeP$_f$-1 nanocomposites, and literature values for CePO$_4$[45]

PPY/CeP$_f$-p			PPY/CeP$_f$-1			CePO$_4$[45]	
2θ/degrees	d/Å	I/I_o (%)	2θ/degrees	d/Å	I/I_o (%)	d/Å	I/I_o (%)
13.79	6.42	23	14.10	6.28	10	6.08	50
19.30	4.60	30	19.69	4.51	19	4.40	30
24.52	3.63	48	24.86	3.58	45	3.53	50
28.48	3.14	100	28.77	3.10	100	3.04	100
30.57	2.93	48	30.88	2.90	40	2.85	40
—	—	—	—	—	—	2.77	—
37.00	2.43	15	37.33	2.41	13	2.37	20
38.30	2.35	14	38.50	2.34	14	2.30	30
39.90	2.26	11	41.04	2.20	64	2.21	—
40.77	2.21	57	—	—	—	—	—
—	—	—	—	—	—	2.16	50
42.76	2.11	03	42.94	2.11	05	2.15	15
43.89	2.06	04	44.30	2.05	06	2.03	03
46.01	1.97	21	46.26	1.96	27	1.94	30
47.74	1.91	52	47.98	1.90	55	1.87	40

View Article Online

Published on 11 April 2003. Downloaded by UNIVERSIDAD ESTADUAL DE CAMPINAS on 05/09/2014 17:47:14.

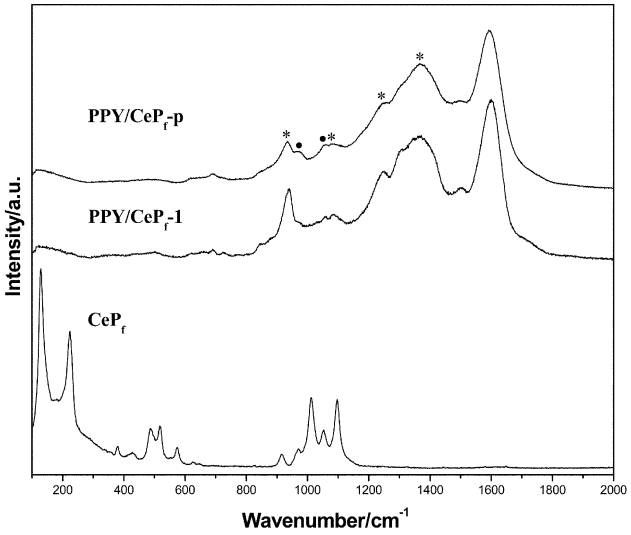

Fig. 3 Raman spectra of PPY/CeP$_f$-p and PPY/CeP$_f$-1 nanocomposites. Bands related to (●) polaron and (*) bipolaron vibrational modes.

band at 950 and another one at 1040 cm^{-1} instead of the bands at 935/970 cm^{-1} and 1059/1087 cm^{-1}, always associated with the oxidized form.[30,46] This result, therefore, is strong evidence of conducting polypyrrole formation.

The band at 1598 cm^{-1} is assigned to the C=C stretching vibrational mode and can be formed from an overlap of bands arising from polaron and bipolaron vibrational modes.[30,46] In Table 3, wavenumber, relative intensity, and tentative vibrational assignments to the Raman bands are summarized.

The coupling of an optic microscope to Raman equipment made it possible to choose specific regions of the samples for Raman spectra acquisition. It was a very useful in the case of the PPY/CeP$_f$-2, PPY/CeP$_f$-3, and PPY/CeP$_f$-4 nanocomposites, where brown "islands" dispersed on the surface of these predominantly yellow samples were observed.

The Raman spectra obtained from these brown "islands" present bands around 1592 and 1345 cm^{-1}, assigned to C=C and C–N stretching vibrational modes, respectively, which means these regions of the samples are related to polypyrrole formation (Fig. 4). Moreover, the spectrum of PPY/CeP$_f$-2 possesses bands at 938, 980 and 1052 cm^{-1}, assigned to polaron and bipolaron vibrational modes, showing the existence of the oxidized polypyrrole form. On the other hand, the spectra of the nanocomposites prepared from lower pyrrole concentrations (PPY/CeP$_f$-3 and PPY/CeP$_f$-4) do not present bands

Table 3 Wavenumber, relative intensity, and tentative vibrational assignments of Raman bands of PPY/CeP$_f$-p and PPY/CeP$_f$-1 nanocomposites, and literature values of the oxidized polypyrrole form[46]

Wavenumber/cm^{-1}			
PPY/CeP$_f$-p	PPY/CeP$_f$-1	PPY[46]	Assignments[a]
1598 vs	1599 vs	1593	νC=C
1501 w	1505 w	1468	νC–N symmetric
1367 s	1371 s	1376	νC–N asymmetric
1302 sh	1310 sh	1327	νC–C
1246 m	1250 m	1235	δC–H (plane) asymmetric
1087 w	1083 w	1086	δC–H (plane) symmetric
1059 w	1061 w	1055	δC–H (plane) symmetric
970 sh	973 sh	973	δ ring
935 m	940 m	933	δ ring
691 vw	690 vw	680	—
620 vw	620 vw	—	—

[a] ν = stretching; δ = deformation; s = strong; m = medium; w = weak; v = very; sh = shoulder.

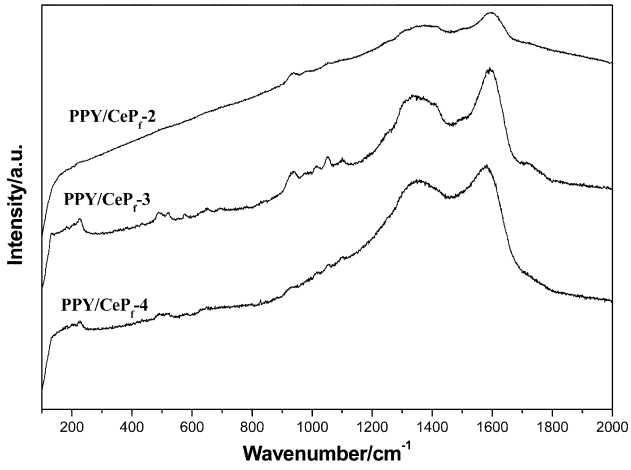

Fig. 4 Raman spectra for the PPY/CeP$_f$-2, PPY/CeP$_f$-3 and PPY/CeP$_f$-4 nanocomposites for the brown "islands".

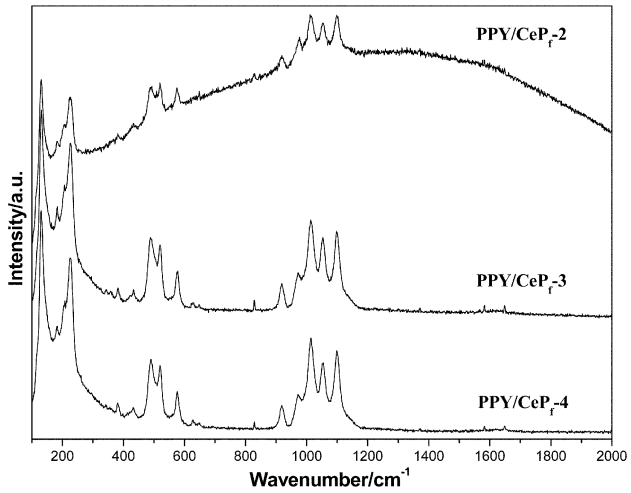

Fig. 5 Raman spectra of the PPY/CeP$_f$-2, PPY/CeP$_f$-3 and PPY/CeP$_f$-4 nanocomposites for the yellow region.

associated with polypyrrole, suggesting only oligomer formation, owing to the presence of the bands related to C=C and C–N stretching vibrational modes. These spectra also show bands assigned to CeP$_f$ vibrational modes, around 226, 490, 520, 576, 1014, 1052 and 1100 cm^{-1}.

Raman spectra obtained from the yellow region of PPY/CeP$_f$-2, PPY/CeP$_f$-3 and PPY/CeP$_f$-4 nanocomposites show bands assigned to the CeP$_f$ vibrational modes (Fig. 5).

These results indicate that the use of lower pyrrole concentrations leads to a small quantity of polymerization initiator sites on the CeP$_f$ attacked by monomers and the polypyrrole formed is not enough to coat the inorganic matrix, as in the case of the PPY/CeP$_f$-p and PPY/CeP$_f$-1 samples.

Scanning electron microscopy

Fig. 6 shows the fibrous morphology of the CeP$_f$ self-supported sheet formed by fibers with thicknesses ranging from 50 to 200 nm.

Scanning electron microscopy images for the PPY/CeP$_f$-p and PPY/CeP$_f$-1 nanocomposites reveal a uniform distribution of the polymer on the inorganic matrix, coating the CeP$_f$ fibers and filling the empty spaces between the fibers (Fig. 7). In spite of the likely conversion of CeP$_f$ to $CePO_4$, whose morphology is not fibrous, the PPY/CeP$_f$-p and PPY/CeP$_f$-1 nanocomposites present fibrous morphology. A possible explanation is that only the CeP$_f$ present on the surface of the fiber is attacked by

View Article Online

Published on 11 April 2003. Downloaded by UNIVERSIDAD ESTADUAL DE CAMPINAS on 05/09/2014 17:47:14.

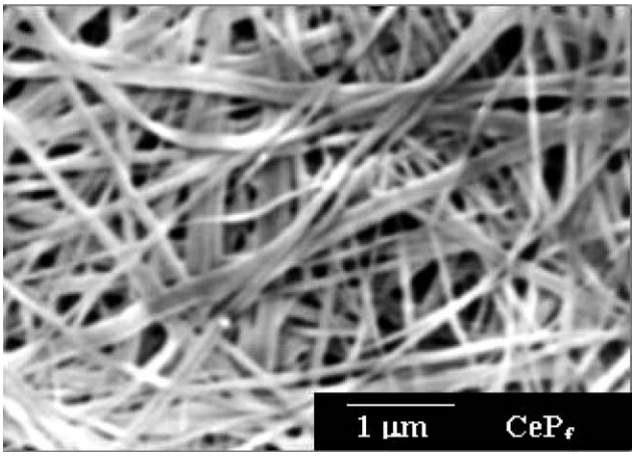

Fig. 6 Scanning electron micrograph illustrating the fibrous morphology of cerium(IV) hydrogenphosphate.

the pyrrole and converted to cerium(III) orthophosphate. The CeP_f existing in the middle of the fiber, therefore, would be preserved, forcing the nanocomposite to keep its fibrous morphology. The fast reaction of pyrrole on the CeP_f self-supported sheets, leading to immediate formation of polypyrrole, may also be responsible for the maintenance of the fibrous morphology and consequent physical integrity of these nanocomposites.

Scanning electron microscopy images for the PPY/CeP_f-2, PPY/CeP_f-3 and PPY/CeP_f-4 nanocomposites show that the polypyrrole was not uniformly distributed on the inorganic matrix. From the electron micrographs of the PPY/CeP_f-3 sample, one can observe that the polymerization takes place on the inorganic matrix fibers and expands to fill the empty spaces existing between the fibers (Fig. 8a). In other regions, a very similar morphology to CeP_f before the pyrrole reaction was observed (Fig. 8b). This information corroborates the results of Raman spectroscopy, which show two kinds of region, one of them presenting the organic phase and the other one without indication of polymer.

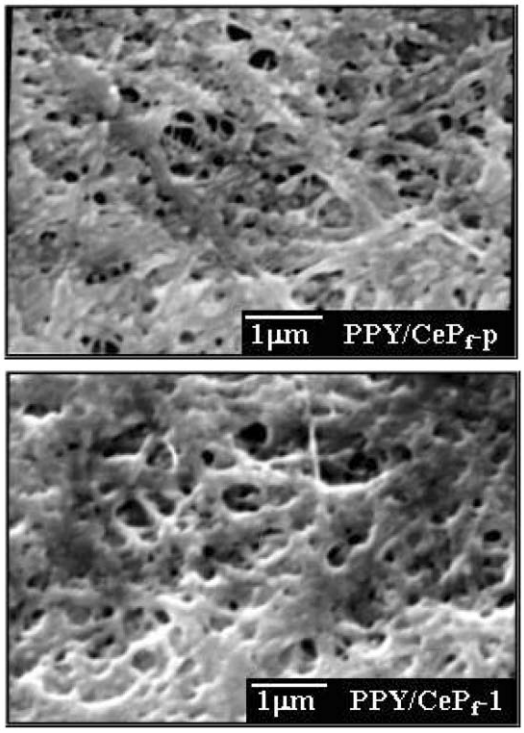

Fig. 7 Scanning electron micrographs of some nanocomposite samples.

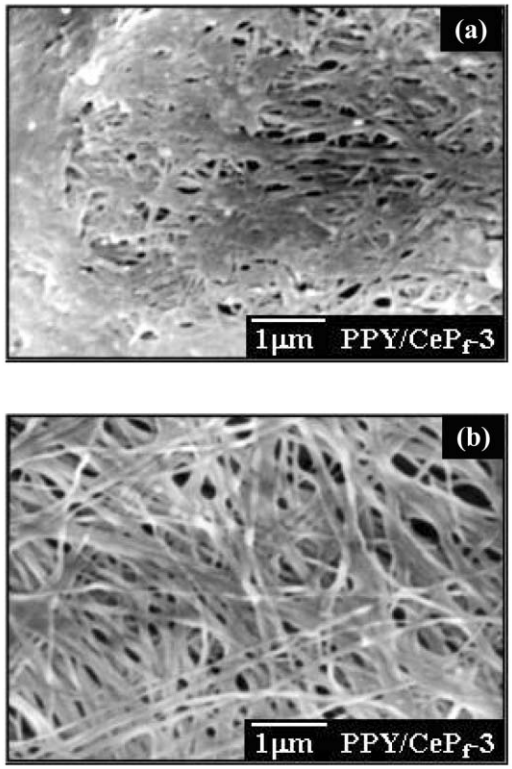

Fig. 8 Scanning electron micrographs of PPY/CeP_f-3, obtained from a region coated by organic phase (a) and without the organic phase coating the fibers (b).

Elemental analysis

The measurements performed for CeP_f shows the absence of C and N, whereas the formation of a very small amount of organic material can be observed for the PPY/CeP_f-2 nanocomposite (Table 4). The amounts of polypyrrole present in the PPY/CeP_f-p and PPY/CeP_f-1 nanocomposites were found to be around 5.80 ± 0.30% and 4.80 ± 0.30% in weight, respectively.

Conductivity properties

The conductivity (σ) was determined from electrical resistance (R) measurements for CeP_f, PPY/CeP_f-p, PPY/CeP_f-1, PPY/CeP_f-2, PPY/CeP_f-3 and PPY/CeP_f-4 samples. Table 5 shows the conductivity values (Ω^{-1} cm^{-1}) obtained for the samples.

In the case of CeP_f, the conductivity measured is in agreement with the literature values that range from 3×10^{-5} to 5×10^{-7} Ω^{-1} cm^{-1}.[35a,47] Polypyrrole conductivity

Table 4 CHN elemental analysis values for the nanocomposite samples

Sample	C (±0.30%)	N (±0.30%)
PPY/CeP_f-2	0.35	0.25
PPY/CeP_f-1	3.66	1.13
PPY/CeP_f-p	4.38	1.42

Table 5 Conductivity values for the nanocomposite samples

Sample	Conductivity/Ω^{-1} cm^{-1}
CeP_f	2×10^{-6}
PPY/CeP_f-4	2×10^{-6}
PPY/CeP_f-3	2×10^{-6}
PPY/CeP_f-2	2×10^{-6}
PPY/CeP_f-1	5×10^{-4}
PPY/CeP_f-p	1×10^{-2}

View Article Online

Published on 11 April 2003. Downloaded by UNIVERSIDAD ESTADUAL DE CAMPINAS on 05/09/2014 17:47:14.

depends on the method of preparation, dopants, medium, *etc.*, ranging from 1×10^{-2} to 3×10^{2} Ω^{-1} cm^{-1}.[48]

A significant increase in the conductivity of the PPY/CeP_f-p sample was observed with respect to CeP_f (4 orders of magnitude). This result confirms the presence of the polypyrrole in its conductive form. The PPY/CeP_f-1 sample presented a lower conductivity than PPY/CeP_f-p, in agreement with the lower amount of polymer in the PPY/CeP_f-1 nanocomposite, as observed by CHN elemental analysis. In the PPY/CeP_f-2, PPY/CeP_f-3 and PPY/CeP_f-4 samples, the measured conductivity presented the same values as CeP_f, owing to the lack of a conducting polymer coating on the inorganic matrix.

Conclusions

Nanocomposite materials consisting of CeP_f self-supported sheets coated by conducting polypyrrole have been prepared *via* chemical oxidation of the pyrrole. When the polymerization takes place, the conversion of fibrous cerium(IV) hydrogenphosphate to cerium(III) orthophosphate is observed, owing to reduction of Ce(IV) ions present in the original inorganic matrix. The preparation of polypyrrole/CeP_f nanocomposites and their properties depend on the pyrrole concentration. It has been shown that pyrrole concentrations lower than 1×10^{-1} mol dm^{-3} are not appropriate to obtain conducting polypyrrole. The maintenance of the integrity of the CeP_f self-supported sheets after pyrrole polymerization makes molded conducting nanocomposites possible.

Acknowledgements

The authors gratefully acknowledge FAPESP, Brazil (process no. 97/2371-1) for financial support.

References

1 R. J. Gehr and R. W. Boyd, *Chem. Mater.*, 1996, **8**, 1807.
2 P. B. Messersmith and E. P. Giannelis, *Chem. Mater.*, 1993, **5**, 1064.
3 L. Wang, J. Schindler, J. A. Thomas, C. R. Kannewurf and M. G. Kanadzidis, *Chem. Mater.*, 1995, **7**, 1753.
4 A. Bhattacharya and A. De, *Prog. Solid State Chem.*, 1996, **24**, 141.
5 F. Leroux and J. P. Besse, *Chem. Mater.*, 2001, **13**, 3507.
6 P. Gomez-Romero, *Adv. Mater.*, 2001, **13**, 163.
7 (*a*) E. Ruiz-Hitzky, *Adv. Mater.*, 1993, **5**, 334; (*b*) E. Ruiz-Hitzky and P. Aranda, *An. Quim. Int. Ed.*, 1997, **93**, 197.
8 (*a*) E. P. Giannelis, *Adv. Mater.*, 1996, **8**, 29; (*b*) E. P. Giannelis, *Appl. Organometal. Chem.*, 1998, **12**, 675; (*c*) R. Krishnamoorti, R. A. Vaia and E. P. Giannelis, *Chem. Mater.*, 1996, **8**, 1728.
9 K. A. Carrado and L. Xu, *Chem. Mater.*, 1998, **10**, 1440.
10 R. Schöllhorn, *Chem. Mater.*, 1996, **8**, 1747.
11 I. F. Gimenez and O. L. Alves, *J. Braz. Chem. Soc.*, 1999, **10**, 167.
12 (*a*) D. J. Maia, O. L. Alves and M.-A. De Paoli, *Synth. Met.*, 1997, **90**, 37; (*b*) A. J. G. Zarbin, M.-A. De Paoli and O. L. Alves, *Synth. Met.*, 1997, **84**, 107; (*c*) A. J. G. Zarbin, M.-A. De Paoli and O. L. Alves, *Synth. Met.*, 1999, **99**, 227; (*d*) A. J. G. Zarbin, D. J. Maia, M.-A. De Paoli and O. L. Alves, *Synth. Met.*, 1999, **102**, 1277; (*e*) A. B. Gonçalves, A. S. Mangrich and A. J. G. Zarbin, *Synth. Met.*, 2000, **114**, 119.
13 (*a*) D. J. Maia, S. das Neves, O. L. Alves and M.-A. De Paoli, *Synth. Met.*, 1999, **102**, 1153; (*b*) D. J. Maia, S. das Neves, O. L. Alves and M.-A. De Paoli, *Electrochim. Acta*, 1999, **44**, 1945.
14 D. J. Maia, A. J. G. Zarbin, O. L. Alves and M.-A. De Paoli, *Adv. Mater.*, 1995, **7**, 792.
15 (*a*) Y.-J. Liu, D. C. DeGroot, J. L. Schindler, C. R. Kannewurf and M. G. Kanatzidis, *J. Chem. Soc., Chem. Commun.*, 1993, 593; (*b*) T. A. Kerr, H. Wu and L. F. Nazar, *Chem. Mater.*, 1996, **8**, 2005; (*c*) T. Challier and R. C. T. Slade, *J. Mater. Chem.*, 1994, **4**, 367; (*d*) C.-G. Wu, D. C. DeGroot, H. O. Marcy, J. L. Schindler, C. R. Kannewurf, T. Bakas, V. Papaefthymiou, W. Hirpo, J. P. Yesinowski, Y.-J. Liu and M. G. Kanatzidis, *J. Am. Chem. Soc.*, 1995, **117**, 9229.
16 T. Bein and P. Enzel, *Angew. Chem., Int. Ed. Engl.*, 1989, **28**, 1692.
17 G. F. McCann, G. J. Millar, G. A. Bowmaker and R. P. Cooney, *J. Chem. Soc., Faraday Trans.*, 1995, **91**, 4321.
18 (*a*) R. Partch, S. G. Gangolli, E. Matijevic, W. Cai and S. Arajs, *J. Colloid Interface Sci.*, 1991, **144**, 27; (*b*) C-L. Huang and E. Matijevic, *J. Mater. Res.*, 1995, **10**, 1327.
19 A. Galembeck and O. L. Alves, *Synth. Met.*, 1997, **84**, 151.
20 S. Maeda and S. P. Armes, *Chem. Mater.*, 1995, **7**, 171.
21 F. Faverolle, A. J. Attias, B. Bloch, P. Audebert and C. P. Andrieux, *Chem. Mater.*, 1998, **10**, 740.
22 A. G. MacDiarmid, *Angew. Chem., Int. Ed.*, 2001, **40**, 2581.
23 A. O. Patil, A. J. Heeger and F. Wudl, *Chem. Ber.*, 1988, **88**, 183.
24 B. F. Cvetko, M. P. Brungs, R. P. Burford and M. Skyllas-Kazacos, *J. Mater. Sci.*, 1988, **23**, 2102.
25 (*a*) J. U. Kim, I. S. Jeong, S. I. Moon and H. B. Gu, *J. Power Sources*, 2001, **97**, 450; (*b*) S. Kuwabata, S. Masui, H. Tomiyori and H. Yoneyama, *Electrochim. Acta*, 2000, **46**, 91.
26 (*a*) S. Mokrane, L. Makhloufi, H. Hammache and B. Saidani, *J. Solid State Electrochem.*, 2001, **5**, 339; (*b*) T. W. Lewis, G. M. Spinks, G. G. Wallace, A. Mazzoldi and D. De Rossi, *Synth. Met.*, 2001, **122**, 379.
27 (*a*) W. A. Gazotti, A. F. Nogueira, E. M. Girotto, M. C. Gallazzi and M. A. De Paoli, *Synth. Met.*, 2000, **108**, 151; (*b*) Y. Z. Hao, M. Z. Yang, W. H. Li, X. B. Qiao, L. Zhang and S. M. Cai, *Sol. Energy Mater. Sol. Cells*, 2000, **60**, 349.
28 G. J. F. Demets, F. J. Anaissi and H. E. Toma, *Electrochim. Acta*, 2000, **46**, 547.
29 (*a*) E. M. Genies and M. Marchesiello, *Synth. Met.*, 1993, **57**, 3677; (*b*) M. V. Deshpande and D. P. Amalnerkar, *Prog. Polym. Sci.*, 1993, **18**, 623.
30 S. Umapathy and R. E. Hester, *J. Mol. Struct.*, 1990, **224**, 113.
31 J. L. Brédas and G. B. Street, *Acc. Chem. Res.*, 1985, **18**, 309.
32 A. Merz, R. Schwarz and R. Schropp, *Adv. Mater.*, 1992, **4**, 409.
33 S. P. Armes, M. Aldissi and S. F. Agnew, *Synth. Met.*, 1989, **28**, C837.
34 A. Clearfield, in *Inorganic Ion Exchange Materials*, CRC Press, Inc., Boca Raton, FL, 1982.
35 (*a*) M. Casciola, U. Constantino and S. D'Amico, *Solid State Ionics*, 1988, **28–30**, 617; (*b*) G. Alberti and U. Constantino, *J. Chromatogr.*, 1974, **102**, 5.
36 G. Alberti, U. Constantino, F. Di Gregorio, P. Galli and E. Torracca, *J. Inorg. Nucl. Chem.*, 1968, **30**, 295.
37 G. Alberti, M. Casciola, U. Constantino and L. Luciani, *J. Chromatogr.*, 1976, **128**, 289.
38 G. Alberti, U. Constantino and L. Zsinka, *J. Inorg. Nucl. Chem.*, 1972, **34**, 3549.
39 H. Hayashi, K. Torii and S. Nakata, *J. Mater. Chem.*, 1997, **7**, 557.
40 D. N. Bernhart and A. R. Wreath, *Anal. Chem.*, 1955, **27**, 440.
41 H. L. Greenhaus, A. M. Feibush and L. Gordon, *Anal. Chem.*, 1957, **29**, 1531.
42 A. Lourenço, Master's Thesis, UNICAMP, Campinas, 1993.
43 (*a*) A. F. Diaz, J. Crowley, J. Bargon, G. P. Gardini and J. B. Torrance, *J. Electroanal. Chem.*, 1981, **121**, 355; (*b*) N. E. Topp, *The Chemistry of the Rare-Earth Elements*, Elsevier Publishing Company, Amsterdam, 1965.
44 G. Alberti and T. Bein, *Solid-State Supramolecular Chemistry: Two- and Three-Dimensional Inorganic Networks*, in *Comprehensive Supramolecular Chemistry*, ed. J. L. Atwood, J. E. D. Davies, D. D. MacNicol, F. Vögtle and J.-M. Lehn, Elsevier Science Inc., New York, 1996.
45 *Powder Diffraction File Search Manual–Inorganic*, Published by the Joint Commitee on Powder Diffractions Standards, Pennsylvania, 1973.
46 (*a*) C. M. Jenden, R. G. Davidson and T. G. Turner, *Polymer*, 1993, **34**, 1649; (*b*) S. J. Vigmond, V. Ghaemmaghami and M. Thompson, *Can. J. Chem.*, 1995, **73**, 1711; (*c*) Y. Furukawa, S. Tazawa, Y. Fujii and I. Harada, *Synth. Met.*, 1988, **24**, 329.
47 P. Barboux and J. Livage, *Solid State Ionics*, 1989, **34**, 47.
48 (*a*) J. L. Brédas, B. Thémans, J. G. Fripiat and J. M. André, *Phys. Rev. B*, 1984, **29**, 6761; (*b*) P. Pfluger, M. Krounbi and G. B. Street, *J. Chem. Phys.*, 1983, **78**, 3212; (*c*) A. Kaynak, *Mater. Res. Bull.*, 1997, **32**, 271.